

First experimental results on High energy density in matter produced by heavy ion beam at the TWAC-ITEP facility

A.Golubev, N.Alekseev, G.Smirnov, M.Basko, N.Borisenko, V.Dubenkoy, A.Fertman, A.Kantsyrev, M.Kats, V.Korolev, T.Mutin, M.Prokuronov, I.Roudskoy, B.Sharkov, V.Turtikov

Institute for Theoretical and Experimental Physics

The expected output parameters of the TWAC (Terawatt Accumulator) facility at the Institute of Theoretical and Experimental Physics (ITEP) in Moscow (the beam power $P_0 = 1$ TW with pulse duration 100ns) provide a possibility to study beam-target interactions for heavy ion inertial confinement fusion [1]. At the end of 2001 the experimental setup for these investigations was successfully assembled and passed its commissioning phase. At the beginning of 2002 the first experiments were carried out with the carbon ion beam. The beamline Fig.1 consists of the eleven standard quadrupole lenses, two dipole magnets, three adjusting magnets and the fine focusing system. The design of the beamline was simulated by the numerical code TRANSPORT [2]. The parameters of the beamline and the final focusing system have been chosen to provide a minimal spot size of the ion beam on target, taking into account the ion beam chromatic aberration.

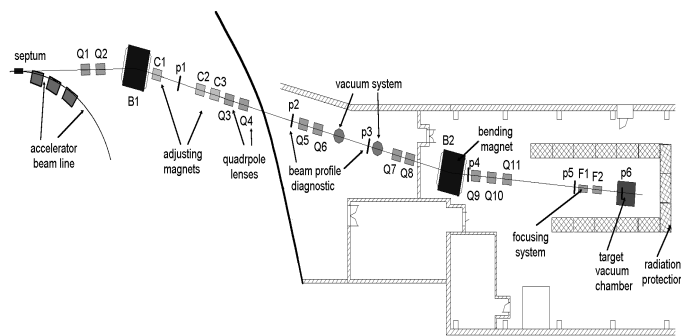
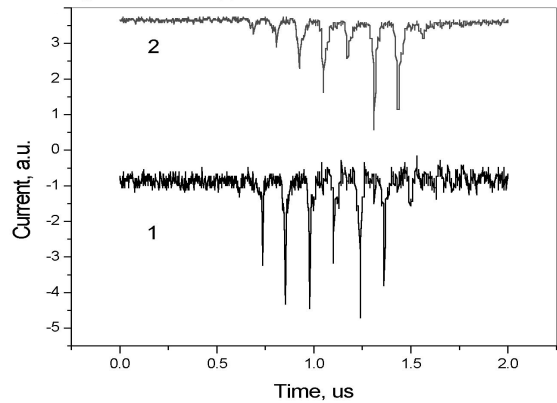


Fig.1.Schematic view of the beamline .

The experimental area consists of a focusing system, a target chamber, a target manipulator and a diagnostic system. The diagnostic system includes the ion diagnostics for ion beam alignments and measurements of ions beam parameters, x-ray and gamma diagnostics as well as particle and optical diagnostics of plasma parameters. The goal of the first experiment was commissioning of the beamline, optimization of the magnetic elements to minimize the focusing spot size of 200 MeV/u carbon ions on the target, and to check the gamma output from the target with the spatial and temporal resolution. The spot size of the ion beam on the target was determined from the images on the scintillator registered by CCD camera. The minimum diameter obtained for the spot size was 1.7mm. Fig. 2 (curve 1) shows a typical signal from the carbon beam measured by the Rogowski coil. The beam intensity in this experiment was $10^7 - 10^8$ particles in 700ns pulse consisting of six bunches of 20ns duration. In the previous works [3] it was shown that monitoring of γ -quantum output arising in nuclear interaction of swift projectile ions with nuclei of a target could be a useful technique for the

diagnostics of high density low temperature non-ideal plasmas. The γ -quantum output not only carries information on

Fig.2. The typical signals from current transformer (1) and gamma-detector (2)



changing of stopping properties of matter during interaction of the ion beam with a target but can also be used for measurements of thermodynamic properties of non-ideal plasma. The main idea consists in measuring the total output of the γ -quanta at energies above 100keV coming from the Coulomb excitation due to rotating and oscillating levels of colliding nuclei with temporal resolution. Very high energies of such γ -quanta allow us to cut off easily other radiation caused by atomic processes using for example a led shield of a few millimeters thickness.

As a first step in realizing the proposed diagnostics, the measurement of gamma output from a thin copper plate of 0.8 mm width moving across the ion beam was performed. Since the total number of γ -quanta is proportional to the number of colliding particles in the interaction region, this output should reflect the ion current distribution over the cross-section of the incident ion beam. Detectors consisting of plastic scintillators and photoelectric multipliers performed the γ -ray registration. The typical gamma output signal from the γ -ray detector and the ion beam pulses measured by the Rogowski coil are presented in fig.2. (curve 1,2). The obtained profile was found to be in close agreement with the image of the beam obtained with the scintillator.

References

- [1] B.Yu.Sharkov, N.N.Alekseev, et al "Heavy ion fusion energy program in Russia" NIM A 464, 2001, pp.1-5
- [2] K.L.Brown at all TRANSPORT CERN 80-04, 1980.
- [3] Yu.N. Cheblukov, et all Dense Plasma Gamma-Ray Diagnostic, 5 International Workshop on Atom Physics for Ion Driven Fusion, Schliersee, 1990, p.3.6.

A method for automatic analysis of experimental data using wavelet transforms

N.A.Borisenko, A.D.Fertman

ITEP, Moscow, Russia

1. Introduction

One among first set of experiments done on TerraWatt Accelerator (TWAC) ITEP was the cross section measurement of secondary nuclei appearance in thin foils. To determine the cross sections Cu and Co targets were irradiated with C^{12} ion beam during several hours. There were accumulated several thousand records. Each record consisted of a set of typically 4-6 (but not greater then 6) peaks of different amplitudes following each other with fixed frequency rate. To solve the stated task it was necessary to identify each peak and find its onset and offset. The complications were that the signal might be corrupted with noise of different types: inducing mapping from magnets and lenses, unknown high frequency distortions and white noise. To parameterize the signal we implemented a technique based on discrete wavelet transform (DWT) [1],[2], which has an advantage over windowed Fourier transform in better time-frequency localization

2. Preliminary signal denoising

In the present work the signal denoising was carried out by means of DWT as considered to be the most powerful and time-frequency localized. The main idea of signal denoising is to decompose signal into wavelets, to identify noise components and to reconstruct the signal without those components [3]. The wavelet used for noise removal was Coiflet K=5 [1]. The scheme applied for threshold selection was SURE [4]. The example of initial and denoised signal fragments are depicted in fig.1.

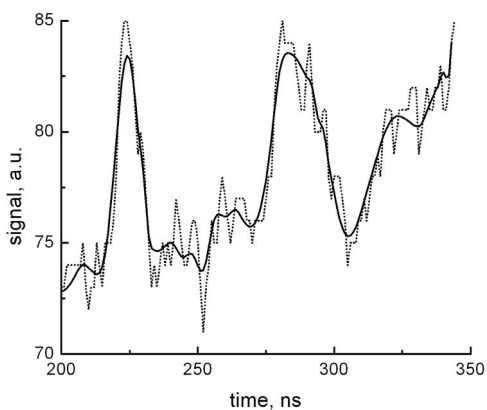


Fig.1 Initial (dotted line) and denoised (solid line) signal

3. Signal parameterization

In the present work the wavelet used for signal analysis was quadratic spline wavelet with compact support. This wavelet is symmetric and it equals to the first derivative of the corresponding scaling function. High pass and low pass and h_k and g_k coefficients can

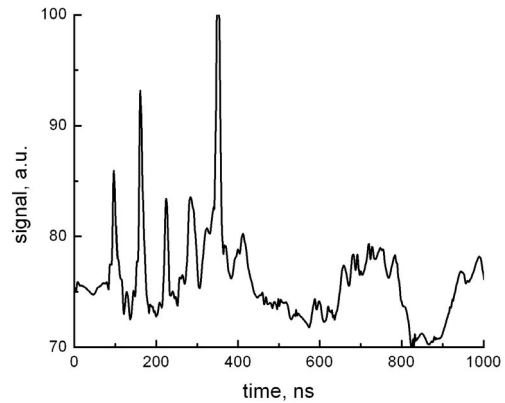


Fig.2 Typical signal to be parameterized

be found in [5]. To parameterize the signal we applied an algorithms described in [6].

4. Results

The example of signal to be analyzed is shown in fig.2. The goal was to detect the position of each actual signal maximum, find onset and offset of each peak and to integrate the signal below each peak. We processed about 1700 records and found that algorithm allows us accurate parameterization of the signal except empty or corrupted records. Even for those data hardly distorted with noise the algorithm allowed us to determine signal maximum position within an uncertainty of 0.07 peak width. The time required for one record processing was about 0.01 seconds, that gives the possibility to use the algorithms in real time data processing. The successful implementation of the described method opens the possibility to use it in other experimental research programs.

References

- [1] I.Daubechie, Ten lectures on wavelets, SIAM, (1992)
- [2] J.C.Goswami, A.K. Chan, Fundamentals of wavelets, John Willey & Sons (1999)
- [3] D.Donoho, Denoising by soft thresholding, IEEE Trans. on Inform. Theory v.41, p.612 (1995)
- [4] P.E.Tikkanen, Nonlinear wavelet and wavelet packet denoising of electrocardiogram signal, Biological Cybernetics, v.80, p.259 (1999)
- [5] S.Mallat, S.Zhong, Characterization of signals from multiscale edges, IEEE Trans on PAMI, v.14, p.710 (1992)
- [6] N.Borisenko, A.D.Fertman, A method for automatic analysis of experimental data using wavelet transforms L&PB to appear (2003)

Optical beam-profile monitoring developed for high intensity proton beam

D.Gardès¹, P.Ausset¹, S.Bousson¹, R.Gobin²
G.Belyaev³, I.Roudskoï³

¹ Centre National de la Recherche Scientifique -Institut National de Physique Nucléaire et de Physique des Particules (CNRS-IN2P3 – Orsay, France)

² Commissariat Energie Atomique (CEA – Saclay, France)

³ Institute of Theoretical and Experimental physics (ITEP – Moscow, Russia)

Abstract : IPHI (Injector of Protons for High Intensity) is foreseen to be the front part of a 1GeV-100mA DC accelerator. Measuring the profile of such an intense beam with an interceptive system is problematic and the study of a new profiler based on hydrogen fluorescence has been tested. The Balmer hydrogen lines were analyzed using a monochromator. The Doppler effect was used to determine in one measurement the different components of the beam (H^+ , $H2^+$, $H3^+$), their relative intensity, energy and spatial extension.

1- Introduction

In the framework of the IPHI (Injector of Protons for High Intensity) demonstrator, which is developed through a CEA– CNRS/IN2P3 collaboration, the SILHI (Source of Light Ions with High Intensities) injector has been producing proton beams since 1996. Beam currents of H^+ up to 120 mA both in cw and pulsed mode are regularly delivered at 95 keV. IPHI is foreseen to be the front end of a future DC accelerator for applications such as Accelerator Driven Systems for nuclear waste transmutation, production of radioactive ion beams or secondary particles.

Even in the low energy part of the machine, classical interceptive diagnostics cannot be used because of the high current densities. With such a beam power, which can reach several kW, non-destructive equipments are required. Optical beam profiling based on the observation of the fluorescence induced by the excitation of molecules or ions is a promising tool for the diagnostics of intense beams [1] D.D. Chamberlin et al. 1981, [2] R.Dölling et al 1997, [3] J.H. Kamperschroer et al. 2000). With this option, there is no influence on the beam propagation by insertion of matter (wire scanning), nor transversal electric field like in a beam profiler based on residual gas ions collection.

2- Experimental method

The light emitted from the interaction of the proton beam with the residual gas results from collisionally dissociation of hydrogen molecules followed by the hydrogen atom excitation. The light was at first recorded with an intensified numerical CCD camera coupled with a large angle optical system to the interaction area. The camera operates within the visible wavelength region (200-820 nm) and was able to detect photons emitted from hydrogen radiative decay (Balmer lines; H_{α} : 656.2 nm, H_{β} : 486.1 nm and H_{γ} : 434.0 nm).

Two orthogonal cameras were installed in order to cover both vertical and horizontal beam profiles. The CCD matrix was cooled at $-45^{\circ}C$ in order to improve the signal-to-noise ratio. Specific software allowing background subtraction, vertical and horizontal projection and peak fitting convolution were used to analyze the results. In a second step, the CCD matrix was installed in the focal plane of an imaging spectrograph equipped with a 900 gr/nm grating. The resolution of the monochromator was better than 0.2 nm at 500 nm wavelength.

3- Direct beam-profile measurements

The residual gas in the beam line is essentially hydrogen at a pressure of 0.5 mPa. The evolution of the profile characteristics has been studied versus the nature of the residual gas. H, N, Ne, Ar, Kr and Xe have been used in a pressure range between 0.5 to 50 mPa . All gases give the same geometrical profile at a given pressure. The light intensity varies linearly with the gas pressure [4] P.Ausset et al 2002).

A comparison, at low intensity, with standard profile-grid system has shown large discrepancies in the profile width determination (fig 1).

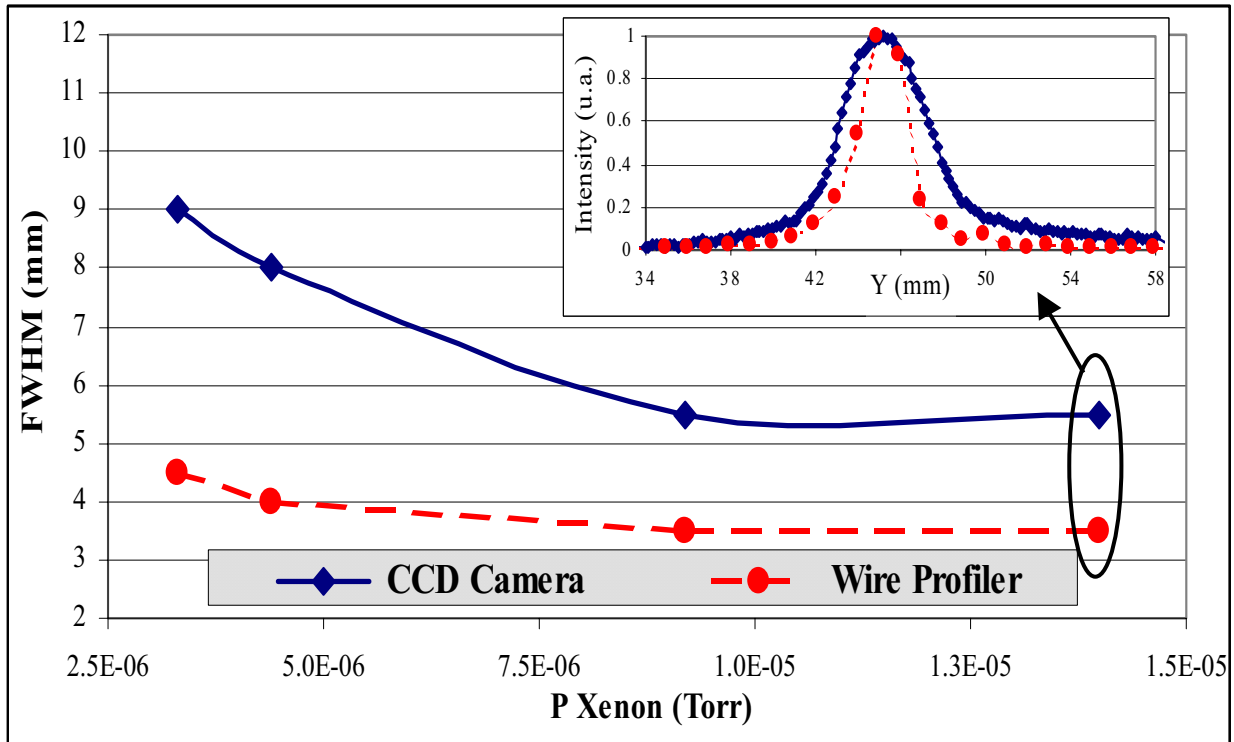


Figure 1 : Comparison between wire scanning profile and fluorescence profile (FWHM) for several Xe gas pressure.

The width of the light emission was larger than the corresponding wire scan. This has been attributed to the existence of a “halo” around the main trajectory. This phenomenon could be explained by delta electrons ejected by primary impact between incident proton and residual gas molecules electrons with a sufficient energy (greater than 16.6 eV) to excite hydrogen atom outside the main beam track. This contribution has been estimated to 6% of the total light yield [5] B.Pottin 2001). Another possibility is an emission from atoms ejected by recoil after the collision with the proton projectiles. A more complete investigation has been done using the wavelength discrimination.

4- Monochromator beam-profile measurements

The beam delivered by the SILHI source includes H^+ , H_2^+ and H_3^+ components. The emission of Balmer lines from H_2^+ and H_3^+ results from their dissociation in Hydrogen atoms, electronic capture and de-excitation following the general scheme :

$\underline{H}_2^+ + H_2 \rightarrow \underline{H} + \underline{H}^* + H_2^+$ or $\underline{H}_3^+ + H_2 \rightarrow [\underline{H}\underline{H}] + \underline{H}^* + H_2^+$, where the star * indicates an excited atom. Atomic emission from H^+ results from an electron capture, followed by excitation and radiation decay process. $H^+ + H_2 \rightarrow H^* + H_2^+$

The hydrogen atoms issued from the main beam H^+ or from the breaking of the H_2^+ and H_3^+ (secondary beams which are also delivered by the ion source), have different velocities and can be discriminated by their wavelength Doppler shifts. $\Delta\lambda \cong \lambda_0 \cdot v/c \cos\theta$, where v is the H^* velocity and θ the angle of observation.

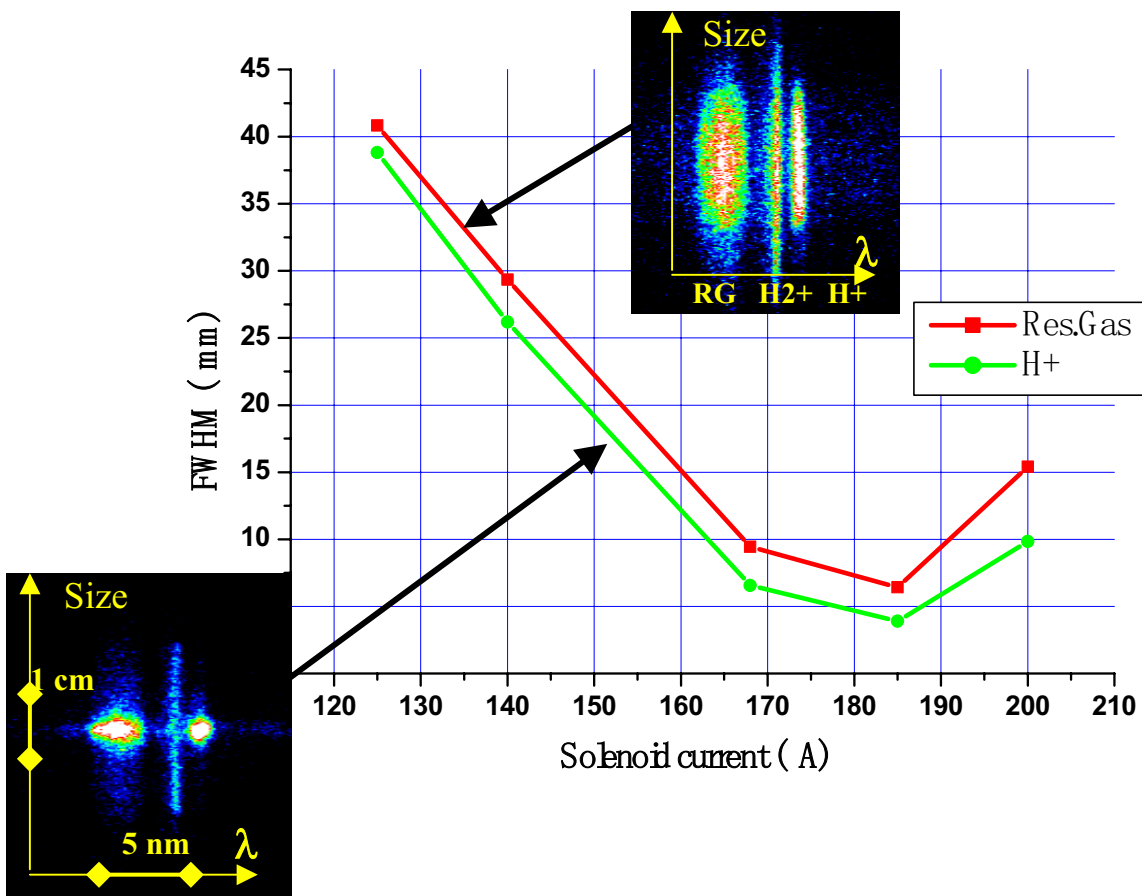
This allows us to identify the components of the beam and their relative intensities.

The electronic capture is the result of a two step process and its probability decreases drastically with the proton velocity. This is a strong limitation to the method. For energies higher than 200 KeV proton, we have to introduce high Z elements in the vacuum chamber in order to reinforce the capture probability. A small amount of Krypton gas (0.1 pa) allows to increase the capture cross sections by 6 order of magnitude on a large range of velocity [6] A.S.Schlachter 1983).

The so called “residual gas” emission corresponds to the beam-induced fluorescence after breaking of the residual background of H₂ gas molecules and their excitation. As a consequence of these different mechanisms, the width of the lines are not the same for the excited residual gas and for the ions in flight. The wavelength broadening associated to the residual gas emission can be attributed to collisionnally dissociated hydrogen molecules projected by recoil. This broadening is also observed when the monochromator is set up at 90° relatively to the beam propagation, measuring only the Doppler effect related to the transverse motion.

The beam profile is extracted from the entrance slit image of the monochromator which is also able to deliver a geometrical information of the beam dimension in the slit orientation. The projection of the vertical image gives the vertical profile of the beam.

As an example, the variation of the beam focusing, obtained by varying a solenoid current, is reported on fig 2 as a function of the Full Width Half Maximum (FWHM) of the residual gas profile and of the H⁺ component. At the diagnostic chamber location the beam diameter evolves from 5 to 40 mm. This allows us to define the size of the « halo » around the main beam. It can be noticed that this halo does not depend on the size of the beam.



656.2 (H α)

Figure 2 : FWHM of H⁺ and residual gas profiles (vertical projection of the Doppler image) for different focusing configuration. The intermediate line (H₂⁺) has not been reported on the graph.

The evolution on the profile characteristics has been studied varying the nature of the residual gas. H, N, Ne, Ar, Kr and Xe have been used in a pressure range between 5 to 10 mPa. Fluorescence yield increases linearly with the gas pressure excepted for hydrogen where we can observe a saturation which have been attributed to an auto-absorption process [4] P.Ausset et al 2002).

5- Conclusion

This measurement has proven to be a powerful method to determine simultaneously several relevant parameters of the high intense proton beam at low energies i.e. energy, composition and relative intensity of the parasitic components, profile in one direction for all the components.

References :

[1] D.D. Chamberlin et al. "Non interceptive transverse beam diagnostics"
IEEE Transactions on nuclear science, Vol N.S.28, N° 3, June 1981

[2] R.Dölling, L.Wicke, J.Pozimski, M.Sarstedt, H.Klein "Optical beam-profile measurement using an intensified CCD camera" GSI Report -97-08 p 47

[3] James H. Kamperschroer et al.. "Initial operation of the LEDA Beam-Induced fluorescence Diagnostic"
Beam instrumentation workshop 2000 - A.I.P.conference proceedings 546

[4] P. Ausset, S. Bousson, D. Gardès, A.C. Mueller, B. Pottin, R. Gobin, G. Belyaev, I. Roudskoy "Optical transverse Beam Profile Measurements for High Power Proton Beam" - EPAC Conf 2002, to be published

[5] B.Pottin, PHD Thesis
Université Paris XI, oct 2001

[6] A.S. Schlachter, J.W.Stearns, W.G.Graham, K.H.Berkner, R.V.Pyle and J.A.Tanis
Phys.Rev. A 27,3372 (1983)

Potential Roles for Heavy Negative Ions as Driver Beams

L. R. Grisham
Plasma Physics Laboratory
Princeton University
P.O. Box 451, Princeton, N. J. 08543, U.S.A.

Abstract

We have performed an initial assessment of the feasibility of producing heavy negative ion beams as drivers for an inertial confinement fusion reactor. Negative ion beams offer the potentially important advantages relative to positive ions that they will not draw electrons from surfaces and the target chamber plasma during acceleration, compression and focusing, and they will not have a low energy tail. Intense negative ion beams could also be efficiently converted to atomically neutral beams by photodetachment prior to entering the target chamber. Depending on the target chamber pressure, this atomic beam will undergo ionization as it crosses the chamber, but at chamber pressures at least as high as 1.3×10^{-4} Torr, there may still be significant improvements in the beam spot size on the target, due to the reduction in path-averaged self-field perveance. The halogens, with their large electron affinities, are the best negative ion candidates. Fluorine and chlorine are the easiest halogens to use for near-term source experiments, whereas bromine and iodine best meet present expectations of driver mass. With regard to ion sources and photodetachment neutralizers, this approach should be feasible with existing technology. Except for the target chamber, the vacuum requirements for accelerating and transporting high energy negative ions are essentially the same as for positive ions.

I. Introduction

Some years ago, we suggested that, for appropriately low pressures within an inertial confinement target chamber, it might be feasible to produce GeV-range atomically neutral driver beams formed from negative ions which were neutralized by photodetachment just prior to the target chamber (Grisham 2001). An advantage of this approach would be that that a negative ion beam would not be subject to electron contamination during acceleration, compression, and focusing, which might be a challenging problem for positive ion beams (Lee 1999). An additional advantage would be that, depending upon target chamber pressure, an atomic beam might not be subject to strong space-charge forces or plasma instabilities until it became photoionized by x-rays relatively close to the target. We have performed an initial assessment of the practicality of producing and utilizing heavy negative ion beams (Grisham 2002). The critical issues are the choice of beam element, ion source, photodetachment neutralizer, vacuum requirements in the accelerator and beam transport system, and reionization of beam particles by background gas in the target chamber.

II. Beam Element and Ion Source

Any element with a finite electron affinity (the binding energy of an added electron) can be used to produce negative ions. However, a practical heavy ion fusion source utilizing many merging beamlets will probably require a current density of roughly 100 mA/cm^2 (Kwan et al 2001). While there are many electronegative elements, only the halogens have sufficiently large electron affinities to render current densities of this magnitude likely. Four of the halogens have exceptionally high electron affinities: fluorine (3.45 eV), chlorine (3.61 eV), bromine (3.63 eV), and iodine (3.06 eV). The first two of these exist as diatomic gases at room temperature, and the latter two form diatomic vapors at moderately elevated temperatures. Consequently, it should be relatively straightforward to produce usefully high current densities of negative ions of any of these halogens over large areas with plasma sources similar to those used to produce beams of positive ions. Experience in the semiconductor industry has shown, for instance, that the majority ion species in chlorine discharges is Cl^- at moderate arc power densities and a pressure of 10 – 20 millitorr (Donnelley 2002). Unlike hydrogen, which has an electron affinity of only 0.75 eV, halogens do not require the addition of cesium to augment negative ion production.

Accordingly, properly optimized, the available current densities of these halogens should be similar to positive ion current densities that could be achieved with elements of similar masses. Under these conditions, the current density which can actually be extracted will be determined by the strength of the extraction electric field, which will be a function of the extractor design. Thus, for optimized negative ion sources, the beam current density should be similar to that which would be achieved with a positive ion of similar mass. Since the negative ions are formed by dissociative attachment, the temperature of the negative ions should not be appreciably higher than the temperature for corresponding positive ions, although this will need to be determined by emittance measurements. As is the case with positive ions, the beam rise and fall times will be determined by the speed of the high voltage switching.

Unlike a positive ion source, a negative ion source requires the application of techniques to suppress the co-extraction of electrons with the negative ions. In the absence of any electron suppression, the extracted electron current exceeds the negative ion current by the ratio of the mobilities of the two species; for similar temperatures this is proportional to the square root of their masses, a large number. This is a problem which has been dealt with for years in the realm of high-current negative deuterium ion sources used for magnetic confinement fusion (Kuriyama 1997). Magnetic fields, which have very little effect on the massive ions, but a large effect on the electrons, along with bias voltages of a few volts between the plasma and the first electrode, can reduce the electron component to a small fraction of the ion current by the time the beam leaves the first extractor stage.

While bromine, with a mass of 81 amu, and iodine, with a mass of 127 amu, are the most likely candidates for a heavy ion driver, a proof-of-principal experiment could be carried out with fluorine or chlorine, which would be valid models for the heavier halogens because they have similar electron affinities and chemistry. These gases are toxic, but less so than some gaseous feedstocks commonly used in the ion implanter industry.

III. Photodetachment Neutralizers

Although negative ion beams are appealing even if they are not neutralized because they avoid the problem of electron accumulation which is endemic to positive ions, they could also be converted to atomic neutrals just prior to entering the target chamber by neutralizers which would be a very small part of the overall heavy ion driver system. Hydrogen negative ions can be converted to neutrals in gas cells with efficiencies of 60%, but gas cells result in low efficiencies for heavier negative ions due to the prevalence of multi-electron-loss events (Grisham et al 1982). Fortunately, photodetachment neutralizers, which were considered long ago for the magnetic confinement fusion beam program Fink et al 1979), are well suited to the characteristics of heavy ion driver beams. By choosing a photon energy which is greater than the electron affinity of the beam element, but much less than the ionization energy of the next electron, it should be possible to approach 100% atomic neutralization. Photodetachment neutralizers, which would use intense laser beams in mirrored cells, are best suited to high-power-density, short-pulse beams. These characteristics are much better typified by heavy ion drivers than they were of magnetic confinement heating beams.

Although the data base for photodetachment cross sections is limited, the cross section generally rises steeply at photon energies just slightly greater than the binding energy of the extra electron, and then varies weakly with photon energies more than 0.2 – 0.4 eV above the binding energy. A wavelength shorter than 0.34 microns will be adequate to photodetach any of the halogen negative ions. Two well developed laser systems, KrF and xenon, are capable of this. According to the Plasma Formulary (2000 edition), the pulsed power levels available in 1990 were in excess of 10^9 watts for KrF lasers, and greater than 10^8 watts for xenon lasers. At that time, the best efficiencies of these lasers were 0.08 for KrF and 0.02 for xenon. Achieving the laser lifetime required for heavy ion drivers may require additional development, since these high power lasers have not been used for many millions of shots.

Although the amount of laser power required to photodetach an ion beam will depend on many details, such as the beam diameter and spacing, and mirror reflectivities, we can examine a simplified example to assess whether existing laser technology is likely to be qualitatively adequate. Consider an I beam pulse with a 1 cm^2 cross section and a length of 10 nanoseconds. Although we don't currently have data on the cross sections of beams we would like to use, data and calculations for a variety of other negative ions in Massey (1976) show photodetachment cross sections varying in the range of $1 \times 10^{-17} \text{ cm}^2$ to $2.4 \times 10^{-16} \text{ cm}^2$. For this example, we choose the bottom of this range, $1 \times 10^{-17} \text{ cm}^2$. The 4.7 eV photons of a KrF laser should be very suitable for photodetaching I, which is bound by 3.06 eV. The line density (LD) of 4.7 eV photons required to neutralize a fraction n_f of a 4 GeV negative-ion beam of iodine per cm of beam width, is given by the expression (Grisham 2002):

$$LD = 6.02 \times 10^8 \ln(1/(1-n_f)) \text{ watts/cm.}$$

The beam current normally does not appear in photodetachment neutralizer formulas because the ion beam is optically thin. In this example, neutralizing 99% of the beam will require a line density of 2.77×10^9 watts/cm. If we use a 20 nanosecond pulse to neutralize a 10 nanosecond ion beam pulse by maintaining this line density across a beam diameter of 3 cm, the required laser energy in a pulse is 166.2 joules. With mirrors

allowing 100 low-loss reflections, which should be readily available, the energy requirement drops to 1.7 joules at a laser power of 2.77×10^7 watts/cm. Light travels 6 meters in 20 nanoseconds, enough time for 150 transits along a 4cm bounce path. With a laser efficiency of 0.08, the required input power to the laser is 21 joules. Although this example is greatly simplified, it does appear that a photodetachment neutralizer should be feasible.

IV. Beam Reionization

At low energies of a few tens of keV/amu, the cross-sections for stripping a negative ion to a neutral are larger than those for neutralizing a positive ion, so the quality of the vacuum in the immediate vicinity of the source is more important for a negative ion beam. Because the halogen negative ions are more than 4 times more strongly bound than D^- , low energy stripping should be less of an issue than it is for deuterium, which is commonly used for large negative ion beams. Moreover, the feedstocks for bromine and iodine, the most probable negative ion drivers, will probably be metal vapors, which can be very quickly pumped. An advantage of negative ions relative to positive ions is that if a negative ion is stripped to a neutral while being extracted from the source, it is unlikely to be converted back to a negative ion through collisions with gas in the initial electrostatic accelerator; thus, a lower energy negative ion tail should not arise, as might happen with positive ions. Having no energy dispersion on the beam going into the main accelerator is a desirable characteristic.

A more serious consideration is the vacuum requirement for the vastly longer path length of the high energy beam through the induction linac, drift-compression region, and final focus optics. As an example, we consider a path length of 1 km, and we take the ionization cross-section to be $6 \times 10^{-16} \text{ cm}^2$. The cross section is an estimate for ionization of Br^- at 20 MeV/amu striking molecular nitrogen (Kaganovich 2002), using a model calibrated from the experiments in Ref. (Mueller et al 2001). At higher energies, the cross section would decline, reaching about $4 \times 10^{-16} \text{ cm}^2$ at 40 MeV/amu. In order to lose less than 0.5% of the beam across a 1 km flight path, the pressure should be no higher than 2.5×10^{-9} torr. For a system this large, this pressure is probably challenging, but not prohibitive.

In any event, the high-energy vacuum requirement for negative ions should not differ by a large factor from whatever is determined to be necessary for singly-charged positive ion beams. This arises from the observation that at higher energies of 100s of keV/amu to 10s of MeV/amu, the positive ions are themselves subject to ionization to higher charge states, with total cross sections that are probably only modestly smaller than for the negative ions. One can see this readily from the fact that the translational kinetic energy of the electrons is larger than the binding energies for most of the electrons in the projectile's electron cloud, not simply the extra electron of the negative ion. For example, at an energy of just 1.4 MeV/amu, the translational kinetic energy of the bound electrons is 0.76 keV.

Beam-beam collisions along the path of an induction linac and the drift compression region after it can also be a loss term for either positive or negative ions. However, this should be a minor (less than 1%) effect for path lengths of a few kilometers (Grisham 2002).

Whether there will be additional value in neutralizing the negative ion beam just prior to entering the target chamber will depend on the chamber pressure eventually adopted for a reactor. To estimate the target chamber vacuum requirements that would enable an atomic beam to be useful, we consider as an example a 40 MeV/amu bromine beam crossing a 3 meter radius target chamber, with the assumption that the beam total ionization cross section in FLIBE will be about $4 \times 10^{-16} \text{ cm}^2$, based on a theoretical estimate (Kaganovich 2002) calibrated against the experiments in Mueller et al (2001). To ionize less than 5% of the neutral beam, in which case space-charge effects would be negligible, the pressure should be no more than 1.3×10^{-5} torr. This is a stringent requirement, especially for a target chamber with liquid FLIBE walls and jets. The HYLIFE-II (Callahan 1996) reactor design was expected to have a pressure of 1.7×10^{-3} torr of beryllium difluoride vapor. However, recent work suggests that it should be possible to reduce this pressure by factors of 5 (Molvik et al 2000) or even somewhat more (Molvik 2002) by various means, including the use of some lower temperature FLIBE jets to shield higher temperature flows, and by other measures with different salt mixtures. Reducing FLIBE temperature, however, causes some reduction in thermal efficiency.

It is not necessary to limit beam stripping to 5% in order to appreciably improve the beam dynamics within the target chamber. The self-field perveance, a measure of the influence of the space charge forces upon the eventual spot size, scales as the square of the average charge. Moreover, the effect upon the spot size at the target depends on the distance from the target at which the beam becomes ionized; ionization close to the target produces much less spot size growth than ionization near the chamber entrance. In the absence of space-charge neutralization within the target chamber, if the atomically neutral beam became 50% ionized while traversing a target chamber with uniform vapor density (corresponding to a pressure of 1.3×10^{-4} torr), then the average ionization would be 25%, and the average self-field perveance would be about 5% of what it would have been if the beam had been singly-ionized across the entire flight path. This is a qualitative evaluation; a full comparison would need to include the effects of partial space-charge neutralization by electrons from the chamber gas, as well as the ionization of beam by x-rays close to the target, where the lever arm on space charge effects is short.

V. Conclusion

It appears that bromine and iodine offer the most attractive negative ions for heavy ion beam neutral-atom drivers. However, fluorine and chlorine will be the easiest gases to use for any initial tests of available negative-ion current densities from practical sources. It also appears that modifications of positive-ion source technology are likely to result in adequate negative-ion current densities from these halogens. The requirements for photodetachment neutralizers appear to be fairly moderate, and well within the state of the art, except perhaps with regard to laser lifetime. The negative ion pressure requirements on the accelerators, transport, focusing, and drift-compression regions should be almost identical to the pressure requirements for positive heavy ion beams. Negative ions offer the advantages that they will not draw electrons from surfaces they pass, nor have low energy tails. If electron contamination turns out to be a challenging problem for positive ion beams, negative ions appear to be a practical backup. If photodetachment neutralizers are added, atomic beams can be produced which could be

essentially free of space-charge effects across the initial, and most important, part of their flight path in the target chamber for chamber pressures in the low 10^{-5} torr range, and which could still have much-reduced average self-field perveance, and thus probably a reduced target spot size, for chamber pressures in the low 10^{-4} Torr range.

Acknowledgments

This research was supported by the U.S. Department of Energy. It is a pleasure to acknowledge stimulating conversations with D. Callahan, R. Davidson, J. Kwan, E. Lee, K. N. Leung, G. Logan, and A. Molvik. We appreciate the support of R. McKnight.

References

- Callahan, D. A. 1996, *Fus. Eng. & Design* 32-33, **441**.
- Donnelley, V. M. 2002, private communication.
- Fink, J. H., Barr, W. L., Hamilton, G. W. 1979, *IEEE Transactions on Plasma Science*, vol. **PS-7**, no. 1, 21 –34.
- Grisham, L.R. 2001, *Nucl. Instr. Meth. Phys. Res. A* **464**, 315.
- Grisham, L.R. 2002, to be published in *Fusion Science and Technology*.
- Grisham, L.R., Post, D., Johnson, B., Jones, K., Barrette, J., T. Kruse, T., Tserruya, I., Da-Hai 1982, W., *Rev. Sci. Instr.* **53** no. 3, 281.
- Kaganovich, I. 2002, private communication.
- Kwan, J.W., Ahle, L., Beck, D. N., Bieniosek, F. M., Faltens, A., Grote, D., Halaxa, E., E. Henestoza, E., W. B. Herrmansfeldt, W.B., V. Karpenko, V., Sangster, T. C. 2001, *Nuclear Instruments and Methods in Physics Research A* **464**, 379 –387 .
- Kuriyama, M. 1997, *Proceedings of the 19th Symp. on Fusion Technology* ,Lisbon (16 – 20 Sept 1996), Editors Varandas, C and Serra,F., Elsevier, pp 693-696.
- Lee, E.P. 1999, private communication.
- Massey, H. S. W. 1976, *Negative Ions* (3rd Edition, Cambridge University Press).
- Molvik, A., Moir, R., Jantzen, C., Peterson, P. 2000, *Bull. Am. Phys. Soc.*, **45**, 206.
- Molvik, A. W. 2002, private communication.
- Mueller, D., L. Grisham, L. R., Kaganovich, I., Watson, R., Horvath, V., Zakaras, K., and Armel, M. 2001, *Physics of Plasmas* **8**, 1753.

External Electron Beam Enhancement of the Metal Vapor Vacuum Arc Ion Source

B.M. Johnson¹, A. Hershcovitch¹, A.S. Bugaev², V.I. Gushenets², E.M. Oks², G.Yu Yushkov², V. A. Batalin³, A.A. Kolomiets³, R.P. Kuibeda³, T.V. Kulevoy³, V.I. Pershin³, S.V. Petrenko³, D.N. Seleznev,³
¹BNL, NY, USA, ²HCEI-RAS, Tomsk, RUSSIA, ³IPEP, Moscow, RUSSIA

Conclusive demonstration of electron-beam enhancement of ion charge states for the Metal Vapor Vacuum Arc (MEVVA) ion source was recently achieved using an external electron beam (E-MEVVA) in experiments performed jointly among the Institute for Theoretical and Experimental Physics (ITEP), Moscow, Russia, the High Current Electronics Institute (HCEI), Tomsk, Russia, and Brookhaven National Laboratory (BNL), USA. The E-MEVVA experiments were performed in Moscow and Tomsk with nearly the same design of ion sources. Typical results for indium, lead, and bismuth cathodes yielded maximum ion charge states of In^{5+} , Pb^{7+} , and Bi^{8+} for E-MEVVA, as compared to In^{2+} , Pb^{2+} , and Bi^{2+} for conventional MEVVA operation.

1. INTRODUCTION

The goal of our joint Russia-U.S.A. research effort is to develop reliable and inexpensive heavy ion sources to produce both (1) high ion charge states and (2) intense ion beam currents. While many ion sources have long-been available to achieve one or the other of these goals, the combination had remained elusive – until now. Our recent results reported in Bugaev et al. [1], Batalin et al.[2], and Batalin et al. [3]offer conclusive demonstrations that both goals (1) and (2) above can be realized through electron beam enhancement of the Metal Vapor Vacuum Arc (MEVVA) ion source. This work is an extension of initial E-MEVVA efforts by Batalin et al. [4] in which encouraging indications of higher charge state production were achieved by combining an electron beam, a vacuum arc ion source, and a drift tube.

The recent E-MEVVA investigations were performed jointly among the High Current Electronics Institute (HCEI), Tomsk, Russia, the Institute for Theoretical and Experimental Physics (ITEP), Moscow, Russia, and Brookhaven National Laboratory (BNL), USA. The experiments were performed in Moscow and Tomsk with nearly the same design of ion sources. Substantially higher ion charge states were clearly observed in both experimental set-ups with two different methods of measuring the ion charge state distributions.

2. MOTIVATIONS AND APPLICATIONS

For many applications it is highly desirable to have a source of heavy ion beams that produces both large ion currents and high charge states. The applications which motivate this work include (a) lower-cost ion implantation facilities, (b) an improved heavy ion injector for the Relativistic Heavy Ion Collider (RHIC) at BNL, and (c) inexpensive and reliable ion sources for various approaches to Heavy Ion Inertial Fusion (HIIF).

Typical ion implantation facilities employ a low-charge state ion source and an extraction system to function as a low-energy pre-accelerator, followed by an ion acceleration

column to produce desired higher ion energies. The high voltage power supplies for pre-acceleration and the accelerating column for final acceleration contribute significantly to facility size and cost. For higher-charge state beams a lower-voltage (and therefore cheaper) power supply can produce the same pre-acceleration energy. If the ion charge states are sufficiently high, then the “pre-accelerator” can reach the desired energy without the need for an additional accelerating column. Such “single-stage” acceleration would enable a more compact design for a lower cost facility.

The Relativistic Heavy Ion Collider (RHIC) at BNL is now operational (<http://www.bnl.gov/RHIC>). Initially, the RHIC physics program will concentrate on Au+Au collisions with 100 GeV in each beam. However, Braun-Munzinger [5] noted that there is physics justification for eventually colliding uranium beams in RHIC, because U+U collisions would produce significantly larger energy densities than Au+Au. The existing tandem preinjector is quite adequate and reliable for the Au+Au collision program currently in progress, but the negative ion source used as the tandem injector cannot produce sufficient uranium beam currents for use at RHIC. Electron-beam enhancement of the MEVVA ion source is a viable basis for developing a versatile heavy ion injection system for relativistic heavy ion accelerators.

Parisi et al. [6] described a typical scenario for a HIIF facility using a combination of ion sources, linacs, and a storage ring as a driver. This and similar schemes (e.g., those described elsewhere in these proceedings) involve multiple ion sources, some funneling steps through increasingly larger linacs, and then a main linac to inject the storage ring. The most numerous elements are the large number of ion sources and initial pre-accelerators. The electron-beam enhanced MEVVA is an inexpensive and compact ion source. The high charge states produced allow for higher extraction energies and the elimination of initial linacs before the first funneling step. These two factors should lead to substantial cost savings in some HIIF facility designs.

3. GENERIC MEVVA

Figure 1 illustrates two variations of the generic MEVVA, which is a prolific generator of highly ionized metal plasma from which intense beams of metallic ions are extracted. Brown [7] described the basic MEVVA, which comprises a series of electrodes (usually concentric and separated by ceramic insulators). The commonly used configuration is a solid electrode of the desired metal, followed by a trigger electrode, an anode, and a three-grid extractor system. As indicated in Fig. 1, the anode and plasma expansion regions can be either separate (left) or combined in a hollow anode (right). Triggering of the vacuum arc is accomplished by applying a short high voltage pulse between the trigger

electrode and the cathode across an insulating surface. Vacuum arc discharge occurs due to formation of cathode spots, which are micron-sized spots on the cathode surface characterized by extremely high current densities. Small spots on the cathode material are vaporized and ionized, producing a plasma plume, from which ions are extracted. Although the MEVVA plasma itself is characterized by a high degree of ionization, only low ion charge states are typically extracted. Depending on the cathode material used a conventional MEVVA ion beam has a mean charge state Q of about $2+$.

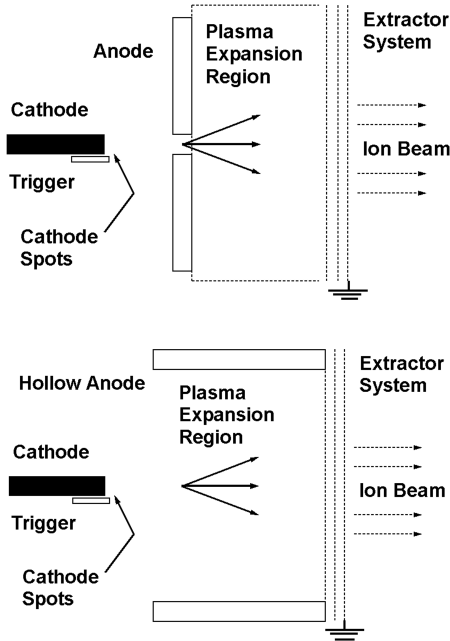


Fig. 1 Schematic layout of a generic Metal Vapor Vacuum Arc (MEVVA) ion source. The two basic variations are: (upper) separate anode and ion drift and (lower) combined anode and ion drift.

4. E-MEVVA

Figure 2 illustrates two variations on the approach of using two MEVVA ion sources to construct an E-MEVVA. The first MEVVA (left) is the electron gun and the second MEVVA (right) is the ionization region. The first variation (upper) is employed in the ITEP-Moscow E-MEVVA, wherein the second MEVVA has a separate anode and plasma expansion (ion drift) region. The second variation (lower) is used in the HCEI-Tomsk E-MEVVA, in which the second MEVVA has a combined hollow anode and ion drift region. In both variations the first MEVVA (e^- gun) uses the combined hollow anode and plasma expansion region. Both ion sources use the same e^- gun MEVVA, which was developed by HCEI-Tomsk. The other difference between the two experimental approaches is that ITEP-Moscow uses magnetic analysis to measure the ion charge state distributions, while HCEI-Tomsk uses time-of-flight. Batalin et al [3] gives more detailed schematic views and layouts, plus full details on the experimental arrangements and operating parameters, which are summarized here in Table 1.

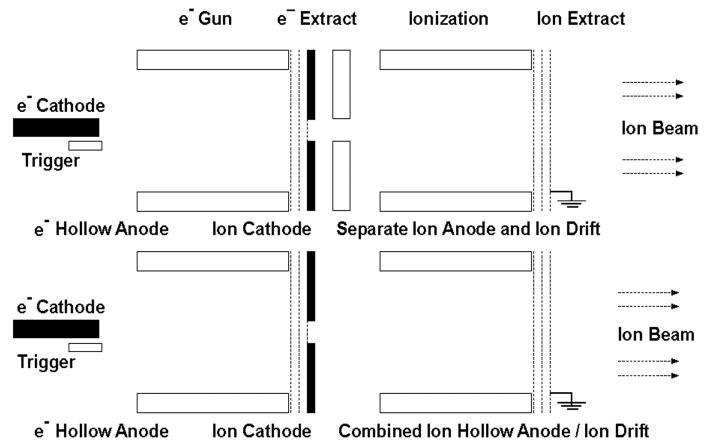


Fig. 2 Schematic layout of E-MEVVA configurations used at ITEP-Moscow (upper) and HCEI-Tomsk (lower).

Table 1. Typical Values of Operating Parameters for the ITEP-Moscow and HCEI-Tomsk E-MEVVA ion sources.

E-MEVVA Operating Parameter	ITEP-Moscow	HCEI-Tomsk
Electron Accelerating Voltage (kV)	18	20
Ion Accelerating Voltage (kV)	50	20
Trigger Voltage (kV)	5	7
Time-of-Flight Gate Voltage (kV)	NA	2
Electron Gun Current (A)	100	200
MEVVA Arc Current (A)	100	300
Ion Emission Current (mA)	20	100-200
Electron Gun Pulse Duration (μ s)	50	100
Vacuum Arc Pulse Duration (μ s)	150	450
Trigger Voltage Pulse Duration (μ s)	10	20
Time of Flight Gate Duration (ns)	NA	100

Herschcovitch et al. [8], Herschcovitch et al. [9], and Batalin et al. [3] discuss the physics considerations for electron-beam enhanced MEVVA operation. Ion charge state distributions are determined by the balance of the electron stripping rate versus the electron capture rate due to charge exchange with neutrals and lower charge state ions. Optimum performance of the E-MEVVA requires sufficient intensity and energy of the electron beam to maximize the ionization rate and to overcome relevant electron binding energies to reach the desired charge states, while at the same time minimizing the production of “fresh plasma” or impurity ion production, which would increase the charge exchange rate and lower the ion beam charge states. The foremost requirement to reduce charge exchange is to improve the vacuum system and the cleanliness of surfaces inside the source to minimize background gas and outgassing. This is necessary, but not sufficient. Batalin et al. [3] documents that the electron gun pulse causes the impurity ion population to increase dramatically due to electrons striking the drift tube walls. Therefore, optimum source performance is achieved when the electron gun pulse is made shorter than the ion arc duration time. This also enables source output optimization by allowing for adjustment of the relative timing of the electron gun pulse within the duration of the ionization arc.

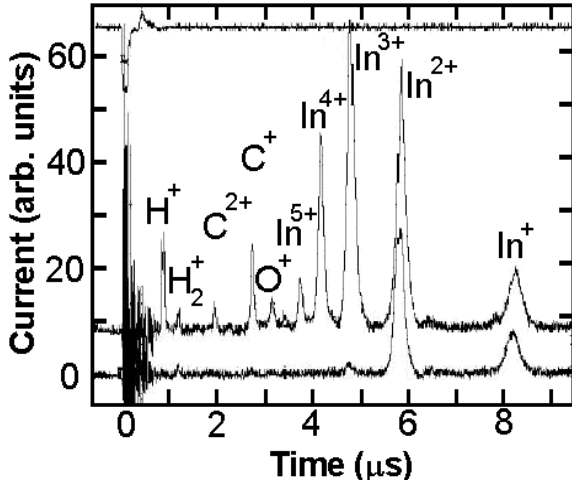


Figure 3 shows a representative HCEI-Tomsk spectrum for E-MEVVA operation with In cathode.

Bugaev et al. [1] showed the HCEI-Tomsk spectra for E-MEVVA operation with Pb cathode. Batalin et al. [2] and Batalin et al. [3] presented the ITEP-Moscow spectra with Pb cathode and the HCEI-Tomsk spectra with Bi cathode. Table 2 gives a comparison of the ionic charge state fractions and mean charge states for all cathode materials studied with the HCEI-Tomsk E-MEVVA. The results are comparable to those obtained at ITEP-Moscow. As shown in the last row of Table 2, the observed increases (ratio of mean charge states) for E-MEVVA versus conventional MEVVA operation ranged from 1.17 for Sm up to 2.50 for Pb.

Table 2. Comparison of ionic charge state fractions (%) and mean charge states $\langle Q_E \rangle$ and $\langle Q_0 \rangle$ for different cathode materials with electron beam off (MEVVA) and on (E-MEVVA). The last line of the table is Ratio of $\langle Q_E \rangle / \langle Q_0 \rangle$.

	Q_0	Cd	In	Sn	Sm	Bi	Pb
M E V V A	1+	44	42	19		19	58
	2+	56	56	76	67	81	42
	3+		2	5	33		
	$\langle Q_0 \rangle$	1.6	1.6	1.8	2.3	1.8	1.4
E - M E V V A	Q_E						
	1+	20	23	5		10	1
	2+	42	39	52	35	18	21
	3+	24	26	21	50	23	35
	4+	11	11	16	12	27	26
	5+	3	1	5	3	14	11
	6+			1		5	4
	7+					2	2
	8+						<1
$\langle Q_E \rangle$	2.3	2.3	2.6	2.7	3.4	3.5	
Ratio	1.44	1.44	1.44	1.17	1.88	2.50	
		Cd	In	Sn	Sm	Bi	Pb

5. CONCLUSIONS

The external electron beam enhanced MEVVA (E-MEVVA) is clearly demonstrated to produce heavy ion beams with

substantially higher charge states than a conventional MEVVA, but with similarly large ion currents. There are many useful applications for such ion sources, including ion implantation, relativistic heavy ion accelerator injection, and heavy ion inertial fusion drivers. In Batalin et al. [3] have reported that performance studies indicate even higher-charge state ions are produced inside the source, but are trapped in the intense electron beam. It may be possible to further optimize the source and to extract even higher charge state ions after the electron beam pulse. Possibilities for future enhancement include (a) increasing the electron beam current and density and (b) further reducing the negative effect of residual gas impurities. The present results already demonstrate that electron beam enhancement of the MEVVA is a viable alternative to other much more costly and difficult to operate devices for the production of intense beams of highly charged ions.

6. ACKNOWLEDGEMENTS

The authors gratefully acknowledge I.G. Brown, and A. Andres, (LBNL, Berkeley) and P. Spadtke, (GSI, Darmstadt) for useful discussions. This work is supported by Research contract between BNL and ITEP with HCEI under the IPP Thrust-1 program, by Russian Foundation of Basic Research under Grant No. 99-02-18163, and by Grant of Russian Ministry of Education for Fundamental Research.

- [1] A.S. Bugaev, V.I. Gushenets, G.Yu Yushkov, E.M. Oks, T.V. Kulevoy, A. Hershcovitch, and B.M. Johnson, *App. Phys. Lett.* 79, 919-921 (2001).
- [2] V.A. Batalin, A.S. Bugaev, V.I. Gushenets, A. Hershcovitch, B.M. Johnson, A.A. Kolomiets, R.P. Kuibeda, T.V. Kulevoy, E.M. Oks, V.I. Pershin, S.V. Petrenko, D.N. Seleznev, and G.Yu Yushkov, *Rev. Sci. Instrum.* 73, 702-705 (2002).
- [3] V.A. Batalin, A.S. Bugaev, V.I. Gushenets, A. Hershcovitch, B.M. Johnson, A.A. Kolomiets, R.P. Kuibeda, T.V. Kulevoy, E.M. Oks, V.I. Pershin, S.V. Petrenko, D.N. Seleznev, G.Yu Yushkov, *Journ. Appl. Phys.* 92, 2884 (2002).
- [4] V.A. Batalin, Y. Volkov, T.V. Kulevoy, S.V. Petrenko, *Proceedings of the 4th European Accelerator Conference (EPAC-94, London, England) 1560-1563 (1994); Proceedings of the 17th International LINAC Conference (LINAC-94, KEK, Ibaraki, Japan) 390-392 (1994).*
- [5] Braun-Munzinger, private communication (1992).
- [6] G. Parisi, A. Sauer, H. Deitinghoff, and H. Klein, *Proceedings of the 19th International LINAC Conference (LINAC-98) 390-392 (1998). Proceedings of the 19th International LINAC Conference (LINAC-98) 390-392.*
- [7] I.G. Brown, *Vacuum arc ion sources. Rev. Sci. Instrum.* 65, 3061 (1994).
- [8] A. Hershcovitch, B.M. Johnson, F. Liu, A. Anders, A. and I.G. Brown, *Rev. Sci. Instrum.* 69, 798-800 (1998).
- [9] A. Hershcovitch, B.M. Johnson, F. Patton, N. Rostoker, A. Van Drie, A. and F. Wessel, *Rev. Sci. Instrum.* 69, 744-747 (2002).

Deuterium targets and the “MDMT” code

A.G. Aksenov,* M.D. Churazov

Institute of Theoretical and Experimental Physics, B. Chermushkinskaya, 25, 117259 Moscow, Russia

Parameter	stages for DT		stages for DD	
	Compression	Ignition	Compression initial → received	Ignition adopted values
ρ_{fuel} , g/cm ³	0.225	100 g/cm ³	0.16 → 100	100
r_{fuel} , cm	0.105	0.005	0.561 → 0.023	0.04
$(\rho r)_{\text{fuel}}$, g/cm ²		0.5		4
ρ_{shell} , g/cm ³	11.4	1000	11.4	1000
r_{DTTablet} , cm				0.005
r_{shell} , cm	~ 0.14	0.015	0.63	0.16
z_{max} , cm	1			
$(\rho l)_{\text{beam}}$, g/cm ²	6			
$J_{\text{beam}}^{\text{max}}$, TW/g	~ 300	4 · 10 ⁶	1230	4 · 10 ⁶
time, ns	~ 100	0.2	250	0.2
E_{beam} , MJ	~ 7	0.4	250	0.4
G	~ 140		3–5	

Table 1: Parameters of DT and DD targets

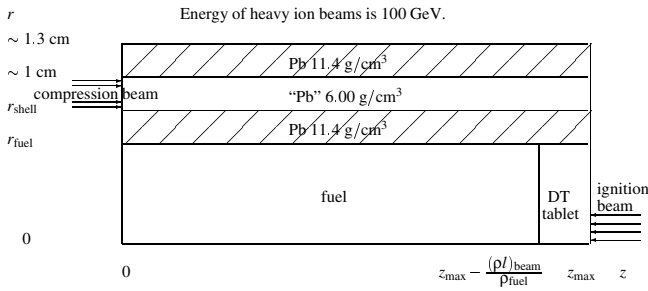


Figure 1: Scheme of cylindrical targets

The DT fuel Heavy Ions Fusion (HIF) conception for a cylindrical target has been analyzed in details in HIF2002 symposium (Basko et al., 2002). This is a cylindrical inertial target with a direct irradiation. On the compression stage, the fuel is compressed by a heavy shell moved into a symmetry axis due to the energy of a hollow beam deposited in a absorber shell. On the next stage the compressed fuel is ignited by an other beam. The ground parameters of the energetic system for the DT project are represented in Table 1, Fig. 1. The requirements for a compression beam for cylindrical target is a similar to those parameters for an indirect spherical target. The parameters of a ignition beam are looked now as enormous. Nevertheless the theoretical investigation of cylindrical targets can be useful (Feoktistov 1998, Atzeni, Ciampi 1999).

To reduce the burning temperature we introduced little amount (10% of ions) of a catalytic ³He into a DD fuel. To keep the same parameters for an ignition beam we used the deuterium tritium tablet irradiated by an ignition beam. We used the two-dimensional approximation (with independent variables r, z in a cylindrical coordinate system) and three temperatures for ions, electrons, radiation (Multi Dimensional Multi Temperatures code by Churazov et al. 2001). Radiation and electron transfers are considered in a diffusion approximation with flux limiters. Instead of the diffusion of charged particles

the local energy deposition is adopted. In some calculations the diffusion of α particles is included. Neutrons are disregarded. The ideal gas law equation of state with $\gamma = 5/3$ for ions and electrons is used. Kinetic coefficients have been taken from one dimensional Deira3 code by Basko 1990. Parameters of a DD target are represented in the table 1. It is no necessity to use a magnetic insulation for $\rho r \geq 2-4$ g/cm².

A cryogenic cylindrical target was considered to obtain the fuel density $\rho \sim 100$ g/cm³ and the target parameter $\rho r \gtrsim 2-4$ g/cm². The scheme of this target is shown at Fig. 1. The beam rotates around the target axis with an enough period to obtain a good axial compression symmetry. The special form of the energy input was introduce at the compression stage of the target $J_{\text{beam}}(r, t) = 12.3 \cdot 10^{14} \left(\frac{t}{10^{-8} \text{ ns}} \right)^5 \frac{\text{erg}}{\text{g} \cdot \text{s}}$ in the “lead” shell with a density $\rho = 6$ g/cm³. In one dimensional calculations of a compression stage by Basko 1990 Deira3 code we received in the final stage the average value of a fuel density $\rho_{\text{fuel}} = 100$ g/cm³ and a fuel radius $r_{\text{fuel}} = 0.023$ cm at an expanses of beam energy 250 MJ (Table 1). For the two dimensional simulation we have taken the received average fuel density but we adopted a more bigger fuel radius $r_{\text{fuel}} = 0.04$ cm³ than a received radius $r_{\text{fuel}} = 0.023$ cm³ while increasing the estimated beam energy for a compression stage $E_{\text{beam}} = 450-750$ MJ. Calculations shows of an existence of a burning wave along a part of a target before the ions temperature reduced to some units of 10^8 K. During this time part of the deuterium fuel burned. The received gain coefficient can be estimated as 3–5. For parameters $r_{\text{fuel}} = 0.08$ cm and $\rho r = 8$ g/cm² estimates give the gain coefficient as about 30.

Our two dimensional calculations shows on the existence of a stationary burning in the deuterium cylindrical targets for parameter $\rho r \gtrsim 8-10$ g/cm² with an attractive gain coefficient ~ 30 and the total energy output ~ 30 GJ. The less level of an energy can be reached only for very high density $\rho_{\text{fuel}} \gtrsim 1000$ g/cm³. But the possibility of an receiving of such densities remains unknown.

The reducing of a parameter ρr to the value ~ 4 g/cm² allow to burn of a fuel part but with an little gain coefficient estimated as 3–5 for $\rho_{\text{fuel}} = 100$ g/cm³. There is an open question about the optimization of a compression to a reducing of the deposited energy.

References

- Atzeni, S., Ciampi, M.L. (1999). Fusion Engineering and Design, 44, 225.
- Basko, M.M. (1990). Nuclear Fusion, 30, 2443.
- Basko, M.M., Churazov, M.D., Aksenov A.G. (2002). “Prospects of heavy ion fusion in cylindrical geometry”. Laser and Particle Beams, 20, 411.
- Churazov, M.D., Aksenov, A.G., Zabrodina, E.A. (2001). Voprosy Atomnoi Nauki i Techniki, ser.: Matem. Model. Fiz. Prozessov, vyp. 1, 20 (in russian).
- Feoktistov, L.P. (1998). Physics-Uspekhi, 41, 1139.

Multigroup kinetic description of x-ray transport in hohlraums.

E.G.Baldina

Elina.Baldina@sunhe.jinr.ru; LHE,JINR,Dubna, Russia

In most of the systems of interest both for IFE research and current and near-future experimental investigations of high energy density in matter (e.g., current experiments with 'nhelix' and future research with 'Phelix' lasers) optical properties of the medium and thermal conditions change both from one region to another and in time. Such research requires high resolution diagnostic methods and advanced numerical techniques.

The kinetic equation of radiation transport.

Consider radiation transport in a hohlraum. The optical properties of the medium vary strongly within the problem. The radiation is absorbed practically completely in a surface layer of the optically thick casing, heating the material. The material under the impact of radiation changes its internal and kinetic energy, starts expanding, and changes its optical properties. In the optically thin interior of the casing (vacuum or filled with low-density and/or low-Z material) radiation penetrates through the whole region with only a small fraction of its energy lost (absorbed and scattered) on the way. In order to adequately describe the above physics, the kinetic equation of radiation transport should be applied in this case:

$$\frac{1}{c} \frac{\partial I_v(\vec{r}, \omega, t)}{\partial t} + \omega \cdot \nabla I_v(\vec{r}, \omega, t) = \varepsilon(\vec{r}, \omega, t) - \kappa_v(\vec{r}, t) I_v(\vec{r}, \omega, t) \quad (1)$$

where t is time, c is light velocity, $I_v(\vec{r}, \omega, t)$ is spectral radiation intensity at point \vec{r} in the direction ω , $\varepsilon(\vec{r}, \omega, t)$ is equilibrium radiation flux at point \vec{r} in the direction ω , $\kappa_v(\vec{r}, t)$ is spectral radiation attenuation coefficient. This equation can have an integrable discontinuous solution, depicting specific features of the system geometry or discontinuities of the boundary conditions.

Treating of discontinuities of boundary conditions and solution with the view factor approach.

Accurate reproduction of specific features of a certain radiation transport problem is often crucial. Two problems having analytical solutions are considered, illustrating the efficiency of the view factor approach.

Radiation transport in a spherical cavity.

Consider a sphere with the surface divided into three parts with different types of boundary conditions: a time-independent radiation source with the flux Q_1 at the fraction of the spherical surface S_1 , the surface S_2 is an absolute diffuse reflector; the surface S_3 is an absolute absorber. This stationary problem has an analytical solution. The temperatures T_1 , T_2 and T_3 depend only on the value of the source flux and the ratios of the surface areas, rather than on the shape and place of S_1 , S_2 and S_3 . For $S_1=S_3$ the stationary temperatures are:

$$T_1 = \sqrt[4]{-\frac{3Q_1}{2} \frac{4}{\sigma c}}, \quad T_2 = \sqrt[4]{-Q_1 \frac{4}{\sigma c}}, \quad T_3 = \sqrt[4]{-\frac{Q_1}{2} \frac{4}{\sigma c}}. \quad (2)$$

The numerical solution precisely follows the discontinuities of the boundary conditions. The average error of the calculated temperature is less than 0.01%, 0.003% and 0.001% for the number of cells on the spherical surface 50, 100, 150, respectively.

Cooling of a sphere.

The 3D problem of cooling of a sphere uniformly filled with radiation corresponding to effective temperature T_0 at the initial moment, has the time-dependent analytical solution [V.A.Karepov, private communication]. The temperature and radiation flux indicatrix at the surface of the sphere is:

$$T(t) = T_0 \sqrt[4]{\frac{1}{2} \left(1 - \left(\frac{c \cdot t}{D} \right)^2 \right)}, \quad \zeta = \begin{cases} const, & \vartheta \geq \vartheta(t), \\ 0, & \vartheta \leq \vartheta(t); \end{cases} \quad \vartheta(t) = \pi - \arccos \left(2 \left(\frac{c \cdot t}{D} \right)^2 - 1 \right) \quad (3)$$

where c is the light velocity, t – time, D – diameter, ϑ - the azimuthal angle, $0 \leq \vartheta \leq \pi$. The accuracy of the numerical solution 1% (20x10 cells) and 0.3% (50x20 cells) is achieved with the view factor method [1,2].

Conclusion.

Modeling of hohlraum systems often requires the solution of Eq.1. The view factor method allows to account for many specific features of such problems (shading, discontinuities of initial and boundary conditions, angular anisotropy, etc.). This approach was successfully used to simulate the x-ray transport experiments on ISKRA-5 (VNIIEF), plasma conditions for possible experiments at Phelix+SIS complex (GSI) [3-5]. Coupled to the kinetic + hydro description of the wall dynamics, it represents a powerful tool for integrated investigation of the systems with strongly inhomogeneous optical properties, e.g. studied presently with nhelix [M.Roth, T.Schlegel, private comm..] and proposed for Phelix+SIS (GSI). The work was partly supported by ISTC 1137 and WTZ 671.98.

References.

1. E.G.Vasina, V.M.Chekshin. *Nuclear Instruments and Methods in Physics Research, A*, 415, 1998, pp.127-132.
2. E.G.Vasina. *GSI Report High Energy Density in Matter Produced by Heavy Ion Beams*, 1997, p.54-55.
3. E.Vasina, V.Vatulin, A.Bazin, G.Skidan, V.Chekshin. *HIF2000*, San Diego, March 2000, *NIMA*, 2001.
4. F.Abzaev, A.Bazin, et.al. *IFSA-99, Bordeaux* pp.279 - 284, 1999.
5. E.Vasina, V.Vatulin *GSI Report High Energy Density in Matter Produced by Heavy Ion Beams*, 2001, p.

